Predicting the solubilities of acetylacetonate-type metal precursors in supercritical CO_2: Thermodynamic modeling using PC-SAFT

Ikuo Ushiki[*,1], Ryo Fujimitsu [1], Azusa Miyajima [1], and Shigeki Takishima [1]

[1] Chemical Engineering Program, Graduate School of Advanced Science and Engineering, Hiroshima University, 1-4-1 Kagamiyama, Higashi-Hiroshima, Hiroshima, 739-8527, Japan

* To whom correspondence should be addressed.
E-mail: iushiki@hiroshima-u.ac.jp Tel : +81-82-424-2052 FAX : +81-82-424-2052

Abstract

The deposition of metal particles on porous supports such as mesoporous silica using supercritical CO_2 has attracted much attention as a method for preparing supported catalysts because the metal particles can be dispersed in the pore structure. Prediction methodology of the solubility of metal precursors in supercritical CO_2 is important to efficiently design the supported catalyst using the supercritical CO_2 deposition method.

In this study, a thermodynamic model using the PC-SAFT (perturbed-chain statistical associating fluid theory) equation of state was used to predict the solubility of various acetylacetonate-type metal precursors in supercritical CO_2. The pure component parameters (the segments number, segment diameter, and dispersion energy) of the metal precursors were determined by considering the correlation with the solubility data of the metal precursors in various organic solvents that were newly measured in this study. The pure component parameters of the metal precursors determined using the correlations were applied to the prediction of the solubility data of metal precursors in supercritical CO_2 using PC-SAFT. The model could reproduce the solubility of various metal precursors over a wide range of temperatures and pressures in supercritical CO_2 without the binary interaction parameter (k_{ij}) for almost all conditions investigated.

Keywords
Supercritical CO_2, Solubility, PC-SAFT

1. Introduction

Methods for depositing metals and metal oxides onto substrates using supercritical fluids as solvents, particularly supercritical CO_2 ($scCO_2$), have attracted increasing attention for preparing supported catalytic metal nanoparticles [1-6] and electronic devices [7, 8]. The use of $scCO_2$ has several important advantages over conventional liquid-solvent methods, such as the solvent power for metal precursors, which can be tuned by adjusting the temperature and pressure, high diffusivity into the microstructure of the substrate, low surface tension, and not requiring a drying process [6, 9].

The $scCO_2$ deposition process consists of three steps [6, 10]: (i) dissolution of the metal precursor into CO_2, (ii) adsorption of metal precursor onto the support, and (iii) calcination and reduction of the precursor to its metallic form. Dissolving a solid metal precursor in $scCO_2$ is the first step in deposition processes using $scCO_2$, and hence, quantifying the metal precursor solubilities is indispensable for designing these processes.

Models using the equations of state can be useful to predict the solubilities of metal precursors in $scCO_2$ in comparison with conventional semi-empirical models such as Chrastil equation [11]. Cubic-type equations of state including the Peng–Robinson equation of state [12] are popular models based on the corresponding-state principle and critical properties (T_c and P_c). However, because the ligand structures of the metal precursors generally decompose at high temperatures, the critical points of metal precursors cannot actually exist; therefore, such cubic-type models are inappropriate for describing the solubilities of metal precursors in $scCO_2$.

Alternatively, statistical associating fluid theory (SAFT)-type equations of state based on molecular thermodynamics combined with perturbation theory [13-16] can be used to predict the solubilities of metal precursors in $scCO_2$. In particular, although several SAFT-type models have been proposed, the perturbed-chain (PC)-SAFT [17, 18] model has been widely applied because of its success in modeling asymmetric systems with complex molecules such as pharmaceuticals [19-21], polymers [22, 23], ionic liquids [24, 25], and deep eutectic solvents [26, 27], including under high-pressure conditions. However, to the best of our knowledge, the application of PC-SAFT for predicting the solubilities of metal precursors in $scCO_2$ has not been investigated in detail except for our previous works [28-30].

Therefore, herein we aimed to predict the solubilities of metal acetylacetonate (acac) precursors in $scCO_2$ using the PC-SAFT equation of state. We first measured the solubilities of metal acac precursors in various pure organic solvents. Then, we fit the solubility of the metal precursors in each pure organic solvent to the PC-SAFT model using the pure-component parameters as adjustable parameters. Finally, we employed the PC-SAFT model to predict the metal precursor solubilities in $scCO_2$ using the pure-component parameters determined by fitting the solubilities of the metal precursors in organic solvents.

2. Experimental

2.1. Materials

$Fe(acac)_3$ (iron(III) acetylacetonate) and $Co(acac)_3$ (cobalt(III) acetylacetonate) (Sigma-Aldrich, USA) with purities of 99 mass%, respectively, were selected as the target metal precursors because reliable data for solubility in $scCO_2$ under a wide range of temperature and pressure conditions for these precursors have been published by Haruki et al. [31, 32]. Three organic solvents, namely, acetone (purity 99.5 mass%), toluene (99.8 mass%), and ethyl acetate (99.5 mass%), which are typical ketone, aromatic, and ester compounds, respectively, were selected as the solvents to dissolve the metal precursors and were obtained from Nacalai Tesque, Japan. All the chemicals were used as received without further purification.

2.2 Measuring the solubilities of metal precursors in organic solvents

The solubilities of the metal acac precursors in each organic solvent were measured based on the method used for solid pharmaceutical compounds reported by Paus et al [33], which were also adopted in our previous work [28] for measuring the solubilities of $Cr(acac)_3$ (chromium(III) acetylacetonate) and $Cu(acac)_2$ (copper(II) acetylacetonate) in the organic solvents. An excess amount of the solid-state metal precursor was added to each pure organic solvent in a 200 cm^3 elementary flask, and the solution was mixed with a magnetic stirrer at atmospheric pressure, and a specific temperature controlled by a water bath. After the system was maintained at a constant temperature for at least 24 h to ensure the thermodynamic equilibrium of dissolution, the magnetic stirrer was stopped for at least 30 min, and a small amount of the supernatant solution in the elementary flasks was sampled and diluted. The concentration of the solute in the supernatant was determined using a UV-vis spectrometer based on pre-prepared calibration curves. The detailed determination method of the solubilities and its validation are reported in elsewhere [28].

3. Model

3.1 PC-SAFT

The PC-SAFT equation of state proposed by Gross and Sadowski [17] is a perturbed-chain representation of the SAFT equation of state developed by Chapman et al. [34, 35]. A brief explanation of PC-SAFT and its pure-component parameters has been provided in this section. The molar residual Helmholtz free energy of the non-associating and nonpolar components is expressed as follows [36]:

$$a^{\mathrm{res}} = a^{\mathrm{hc}} + a^{\mathrm{disp}} \tag{1}$$

where a^{res} represents the residual free energy with respect to an ideal-gas reference, with contributions of hard-chain repulsion (a^{hc}) and dispersion attraction (a^{disp}) arising from van der Waals forces.

Three pure-component parameters must be determined for each component *i* in the PC-SAFT equation of state: segment number m_i, segment diameter σ_i, and segment dispersion energy parameter u_i [17]. The methods used for determining these parameters in the present study are described in 3.2.

The Lorentz–Berthelot combining rules used for unlike pair interactions in a mixture of components *i* and *j* to describe multicomponent systems are as follows [17]:

$$\sigma_{ij} = \frac{1}{2}\left(\sigma_i + \sigma_j\right) \tag{2}$$

and

$$u_{ij} = \left(1 - k_{ij}\right)\sqrt{u_i u_j} \tag{3}$$

To increase the accuracy of the model, the binary interaction parameter (k_{ij}) in Eq. (3) that describes the interactions between components *i* and *j* can be used as a fitting parameter in a fit to the experimental results if necessary [37].

3.2 Determining the PC-SAFT parameters by fitting to the solubility in the organic solvent

The values of the pure-component parameters (m_i, σ_i, and u_i) for all components present in the target system are necessary for the PC-SAFT calculation of the metal precursor solubilities in organic solvents and $scCO_2$. These PC-SAFT parameters are typically determined via regression analysis of the experimentally obtained phase equilibrium properties of pure components, including saturated vapor pressures and liquid densities. The parameters for organic solvents and CO_2 were similarly determined as shown in **Table 1**.

Table 1. PC-SAFT pure-component parameters for CO_2 and the organic solvents used in this work.

Component	m_i [-]	σ_i [Å]	u_i/k_B [K]	Ref.
CO_2	2.6037	2.555	151.04	[38]
Toluene	2.8149	3.7169	285.69	[17]
Acetone	2.8913	3.2279	247.42	[39]
Ethyl acetate	3.5375	3.3079	230.80	[17]

The PC-SAFT pure-component parameters for the metal acac precursors were determined by fitting the parameters to the solubilities of the metal precursors in various organic solvents. Based on the thermodynamic phase equilibrium condition for the solid and liquid phases for which the chemical potentials of the metal precursor in both phases are equal, the metal precursor solubility in the organic solvent (x_{prec}) can be derived as [40]:

$$x_{\mathrm{prec}} = \frac{1}{\gamma_{\mathrm{prec}}} \exp\left\{ -\frac{\Delta h_{\mathrm{prec}}^{\mathrm{fus}}}{RT}\left(1 - \frac{T}{T_{\mathrm{m}}}\right)\right\} \tag{4}$$

where γ_{prec} is the activity coefficient of the metal precursor in the liquid phase, which consists of the dissolved metal precursor and the organic solvent. In Eq. (4), $\Delta h_{\mathrm{prec}}^{\mathrm{fus}}$ and T_{m} are the enthalpy of fusion and melting point of the solid metal precursors, respectively, and these parameters were obtained from the literature [41, 42].

The activity coefficient γ_{prec} in Eq. (4) is defined as the ratio between the fugacity coefficients of the metal precursor in the solvent ($\varphi_{\mathrm{prec}}^{\mathrm{L}}$) and the pure metal precursor in liquid form ($\varphi_{0,\,\mathrm{prec}}^{\mathrm{L}} = \varphi_{\mathrm{prec}}^{\mathrm{L}}\left(x_{\mathrm{prec}} \to 1\right)$), as described by [43, 44]:

$$\gamma_{\mathrm{prec}} = \frac{\varphi_{\mathrm{prec}}^{\mathrm{L}}}{\varphi_{0,\,\mathrm{prec}}^{\mathrm{L}}} \tag{5}$$

The fugacity coefficients are calculated based on the corresponding residual chemical potential ($\mu_{\mathrm{prec}}^{\mathrm{res}}$):

$$\ln \varphi_{\mathrm{prec}} = \frac{\mu_{\mathrm{prec}}^{\mathrm{res}}\left(T, V, x_{\mathrm{prec}}\right)}{RT} - \ln Z \tag{6}$$

where T, V, and Z are the temperature, volume, and compressibility factor of the system, and x_{prec} is the mole fraction of the precursor in the solvent. $\mu_{\mathrm{prec}}^{\mathrm{res}}$ can be obtained from the partial derivative of the residual Helmholtz energy of the system (a^{res}) used in PC-SAFT (Eq. (1)).

The detailed expressions can be found in the original PC-SAFT report [17].

Thus, the solubilities of the metal precursors in each pure organic solvent were calculated using Eq. (4) and fitted to the corresponding experimental solubility data using the three PC-SAFT pure-component parameters (m_i, σ_i, and u_i) for the metal precursors as adjustable parameters while minimizing the average relative deviation (ARD) defined as:

$$\mathrm{ARD}\ [\%] = \frac{1}{ND}\sum_{i}^{ND}\frac{\left|x_{\mathrm{prec,calc},i} - x_{\mathrm{prec,exp},i}\right|}{x_{\mathrm{prec,exp},i}} \times 100 \tag{7}$$

In the fits used to determine the PC-SAFT pure-component parameters for the metal precursors, the binary interaction parameter k_{ij} in Eq. (3) was set to zero. The fitting calculations were performed using the simplex optimization method in MATLAB® 2021a.

3.3 Predicting the solubilities of metal precursors in scCO₂ by PC-SAFT

Based on the thermodynamic relationship expressed using the fugacities of the precursors in the solid and supercritical phases, the solubility of a metal precursor in $scCO_2$ (y_{prec}) can be modeled as [29, 40]:

$$y_{\mathrm{prec}} = \frac{p_{\mathrm{prec}}^{\mathrm{sub}}}{P\varphi_{\mathrm{prec}}^{\mathrm{scf}}} \exp\left[\frac{v_{\mathrm{prec}}^{\mathrm{solid}}\left(P - p_{\mathrm{prec}}^{\mathrm{sub}}\right)}{RT}\right] \tag{8}$$

Here, $v_{\mathrm{prec}}^{\mathrm{solid}}$ is the solid molar volume of the metal precursor, which was taken from the literature [45, 46]. $\varphi_{\mathrm{prec}}^{\mathrm{scf}}$ is the fugacity coefficient of the metal precursor in $scCO_2$, which can be calculated with PC-SAFT according to Eq. (6) using the corresponding chemical potential with the pure-component parameters of each component, as described in section 3.2. $p_{\mathrm{prec}}^{\mathrm{sub}}$ is the sublimation pressure of the metal precursors taken from the literature [47].

The ARD between the predicted and experimental values of the solubilities was calculated according to a formula similar to Eq. (7).

4. Results and discussion

4.1 Measuring and fitting the solubilities of metal precursors in organic solvents

4.1.1 Measured solubilities of metal precursors in organic solvents

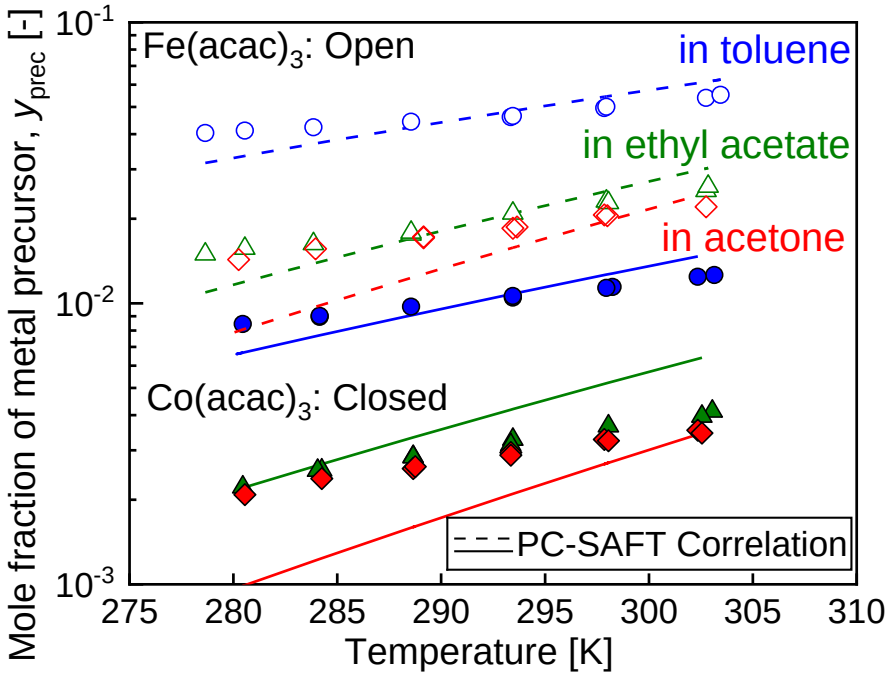

Figure 1. Measurement and correlated results of solubilities of $Fe(acac)_3$ (open symbols and dashed lines) and $Co(acac)_3$ (closed symbols and solid lines) with PC-SAFT at k_{ij} = 0 using the pure-component parameters of the metal precursors as fitting parameters.

Figure 1 shows the measured $Fe(acac)_3$ and $Co(acac)_3$ solubilities in three pure organic solvents, viz., toluene, acetone, and ethyl acetate, and the obtained values. **Figure 1** reveals that the solubility increased with increasing temperature, showing the typical temperature-dependent solubility of solid organic compounds in organic solvents at atmospheric pressure [48]. In the investigated temperature range, the solubilities follow the order of toluene > ethyl acetate ≈ acetone. The higher solubility of this metal precursor in toluene is probably due to the higher affinity of the aromatic compound to the acac ligand.

4.1.2 Results of fitting the solubilities of metal precursors in organic solvents

Table 2. PC-SAFT parameters for metal precursors investigated in this work.

Component	m_i [-][a]	σ_i [Å]	u_i/k_B [K]	ARD [%]
$Fe(acac)_3$	13.652	3.1225	165.77	18.3
$Co(acac)_3$	14.042	3.1852	150.75	26.5

The dashed and solid lines in **Figure 1** correspond to the fitting results for the measured solubilities of the metal precursors in the different pure organic solvents when the three PC-SAFT pure-component parameters were used as the fitting parameters, while k_{ij} in Eq. (3) was set at zero. The PC-SAFT parameters of the metal precursors determined by the fitting are listed in **Table 2** together with the ARD values of the fits. As shown in **Figure 1** and **Table 2**, the PC-SAFT fits can approximately describe the trend in the solubilities of the metal precursors in the three solvents.

4.2 Calculating the solubilities of metal precursors in scCO₂

4.2.1 Predicting the solubilities using PC-SAFT

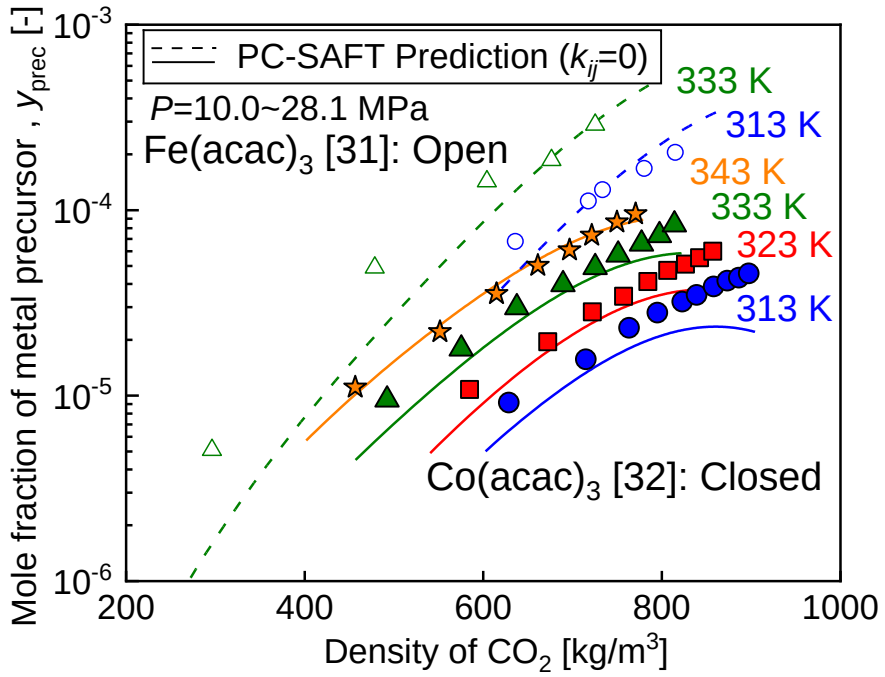

Figure 2. Prediction results of isothermal solubilities of $Fe(acac)_3$ (dashed lines) and $Co(acac)_3$ (solid lines) in $scCO_2$ with PC-SAFT at k_{ij} = 0 as a function of CO_2 density in the pressure range of 10.0 MPa to 28.1 MPa. Symbols: experimental values from Haruki et al. [31, 32] (open: $Fe(acac)_3$, closed: $Co(acac)_3$) at 343 K (★), 333 K (▲), 323 K (■), and 313 K (●).

Table 3. Predicted results of the isothermal solubilities of the metal precursors in $scCO_2$ obtained using PC-SAFT at k_{ij} = 0 at P = (10.0 to 28.1) MPa.

Metal precursors	T [K]	ARD_{pred} [%]
$Fe(acac)_3$	333	58.9
	313	16.2
	overall	37.5

$Co(acac)_3$	343	7.4
	333	21.9
	323	27.3
	313	44.4
	overall	25.3

The dashed and solid lines in **Figure 2** show the predicted isothermal solubilities of $Fe(acac)_3$ and $Co(acac)_3$ in $scCO_2$ as a function of the CO_2 density using PC-SAFT and pure-component parameters of the metal precursors (**Table 2**) determined by fitting to the solubilities in the organic solvents, as mentioned in section 4.1.2. **Table 3** summarizes the ARD values obtained by comparing the experimental and predicted results. As shown by the dashed lines in **Figure 2** and the data presented in **Table 3**, the PC-SAFT predictions reproduced the isothermal solubilities of the metal precursors in $scCO_2$ with ARD values defined by Eq. (7) being less than 30% for almost all the investigated conditions, even though k_{ij} was set at 0 in the combining rule (Eq. (3)).

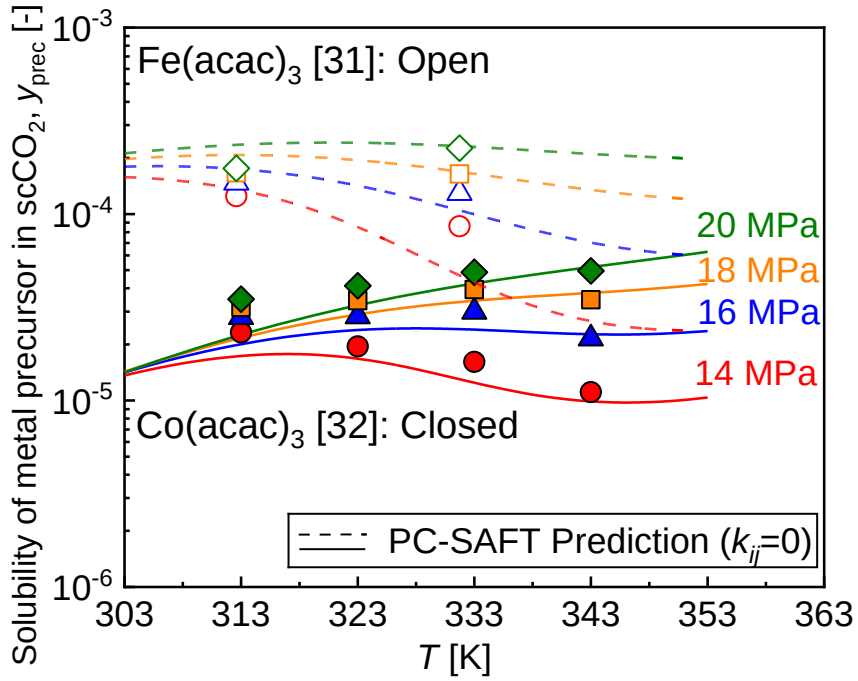

Figure 3. Prediction results of isobaric solubilities of $Fe(acac)_3$ (dashed lines) and $Co(acac)_3$ (solid lines) in $scCO_2$ with PC-SAFT at k_{ij} = 0 as a function of temperature. Symbols: experimental values from Haruki et al. [31, 32] (open: $Fe(acac)_3$, closed: $Co(acac)_3$) at 20.0 MPa (◆), 18.0 MPa (■), 16.0 MPa (▲), and 14.0 MPa (●).

Table 4. Predicted results of the isobaric solubilities of the metal precursors in $scCO_2$ obtained using PC-SAFT at k_{ij} = 0 at T = (313 to 343) K.

Metal precursors	P [MPa]	ARD_{pred} [%]
$Fe(acac)_3$	20.0	28.1
	18.0	19.7
	16.0	14.4
	14.0	19.1
	overall	20.3
$Co(acac)_3$	20.0	18.2
	18.0	17.3
	16.0	17.2
	14.0	18.7
	overall	17.8

The dashed and solid lines in **Figure 3** and **Table 4** show the results of the PC-SAFT predictions for the isobaric solubilities of $Fe(acac)_3$ and $Co(acac)_3$ in $scCO_2$ as a function of temperature from 313 K to 343 K using k_{ij} = 0. The symbols in **Figure 3** indicate the corresponding experimental data that were determined by interpolating and extrapolating from the literature values by Haruki et al. [31, 32] using the spline method. As shown in **Figure 3** and **Table 4**, the isobaric solubilities of the metal pre0cursors in $scCO_2$ can be predicted to within 20% of ARD at almost all conditions.

5. Conclusion

Predictions of the solubilities of two metal acetylacetonates, $Fe(acac)_3$ and $Co(acac)_3$, in $scCO_2$ using the PC-SAFT equation of state were performed. The solubilities of the metal precursors in various organic solvents were measured and used to determine the PC-SAFT pure-component parameters (segment number, segment diameter, and dispersion energy) for the metal precursors. The pure-component parameters of the metal precursors determined with the PC-SAFT fitting were then applied to predict the solubilities of the metal precursors in $scCO_2$ via PC-SAFT. These predictions reproduced the metal precursor solubilities over a wide range of temperatures and pressures under almost all conditions, even though the binary interaction parameter k_{ij} was set to zero in the combining rule. On the other hand, the present method using the original PC-SAFT does not consider the contribution of the polarity of the components, including the quadrupole moment of CO_2. Consequently, a PC-SAFT approach that considers the polarity [49, 50] may improve the results of the calculated solubilities, which will be investigated in the future.

References

[1] I. Ushiki, N. Takahashi, M. Koike, Y. Sato, S. Takishima, H. Inomata, J. Supercrit. Fluid., 135 (2018) 137-144.
[2] I. Ushiki, M. Koike, T. Shimizu, Y. Sato, S. Takishima, H. Inomata, J. Supercrit. Fluid., 140 (2018) 329-335.
[3] I. Ushiki, N. Takahashi, T. Shimizu, Y. Sato, M. Ota, R.L. Smith, H. Inomata, J. Supercrit. Fluid., 120 (2017) 240-248.
[4] T. Shimizu, I. Ushiki, M. Ota, Y. Sato, N. Koizumi, H. Inomata, Chem. Eng. Res. Des., 95 (2015) 64-68.
[5] K. Matsuyama, T. Tsubaki, T. Kato, T. Okuyama, H. Muto, Mater. Lett., 261 (2020) 127124.
[6] I. Ushiki, K. Matsuyama, R.L. Smith, Sustainable Nanoscale Engineering, (2020) 395-414.
[7] S.B. Barim, S.E. Bozbag, H.B. Yu, R. Kizilel, M. Aindow, C. Erkey, Catal. Today, 310 (2018) 166-175.
[8] S.B. Barim, E. Uzunlar, S.E. Bozbag, C. Erkey, J. Electrochem. Soc., 167 (2020) 054510.
[9] S.E. Bozbag, C. Erkey, J. Supercrit. Fluid., 96 (2015) 298-312.
[10] C. Erkey, J. Supercrit. Fluid., 47 (2009) 517-522.
[11] J. Chrastil, J. Phys. Chem., 86 (1982) 3016-3021.
[12] D.Y. Peng, D.B. Robinson, Ind. Eng. Chem. Fundam., 15 (1976) 59-64.
[13] M.S. Wertheim, J. Stat. Phys., 42 (1986) 477-492.
[14] M.S. Wertheim, J. Stat. Phys., 42 (1986) 459-476.
[15] M.S. Wertheim, J. Stat. Phys., 35 (1984) 35-47.
[16] M.S. Wertheim, J. Stat. Phys., 35 (1984) 19-34.
[17] J. Gross, G. Sadowski, Ind. Eng. Chem. Res., 40 (2001) 1244-1260.
[18] J. Gross, G. Sadowski, Ind. Eng. Chem. Res., 41 (2002) 5510-5515.
[19] G. Sodeifian, S.M. Hazaveie, S.A. Sajadian, F. Razmimanesh, Fluid Phase Equilib., 493 (2019) 160-173.
[20] G. Sodeifian, N. Saadati Ardestani, S.A. Sajadian, H.S. Panah, Fluid Phase Equilib., 458 (2018) 102-114.
[21] G. Sodeifian, F. Razmimanesh, S.A. Sajadian, H. Soltani Panah, Fluid Phase Equilib., 472 (2018) 147-159.
[22] K. Gong, S.R. Panuganti, W.G. Chapman, J. Appl. Polym. Sci., 134 (2017).
[23] J. Chmelař, K. Haškovcová, M. Podivinská, J. Kosek, Ind. Eng. Chem. Res., 56 (2017) 6820-6826.
[24] R.I. Canales, C. Held, M.J. Lubben, J.F. Brennecke, G. Sadowski, Ind. Eng. Chem. Res., 56 (2017) 9885-9894.

[25] L.F. Zubeir, T. Spyriouni, D. Roest, J.R. Hill, M.C. Kroon, Ind. Eng. Chem. Res., 55 (2016) 8869-8882.
[26] C.H.J.T. Dietz, J.T. Creemers, M.A. Meuleman, C. Held, G. Sadowski, M. Van Sint Annaland, F. Gallucci, M.C. Kroon, ACS Sustainable Chem. Eng., 7 (2019) 4047−4057.
[27] C. Dietz, F. Gallucci, M.V. Annaland, C. Held, M.C. Kroon, Ind. Eng. Chem. Res., 58 (2019) 4240-4247.
[28] I. Ushiki, R. Fujimitsu, S. Takishima, J. Supercrit. Fluid., 164 (2020) 104909.
[29] I. Ushiki, Y. Sato, S. Takishima, H. Inomata, J. Chem. Eng. Jpn., 52 (2019) 243-252.
[30] I. Ushiki, Rev. High Press. Sci. Technol., 29 (2019) 187-193.
[31] M. Haruki, F. Kobayashi, S.I. Kihara, S. Takishima, Fluid Phase Equilib., 308 (2011) 1-7.
[32] M. Haruki, F. Kobayashi, K. Kishimoto, S. Kihara, S. Takishima, Fluid Phase Equilib., 280 (2009) 49-55.
[33] R. Paus, E. Hart, Y. Ji, G. Sadowski, J. Chem. Eng. Data, 60 (2015) 2256-2261.
[34] W.G. Chapman, K.E. Gubbins, G. Jackson, M. Radosz, Fluid Phase Equilib., 52 (1989) 31-38.
[35] W.G. Chapman, K.E. Gubbins, G. Jackson, M. Radosz, Ind. Eng. Chem. Res., 29 (1990) 1709-1721.
[36] M. Ozturk, S.R. Panuganti, K. Gong, K.R. Cox, F.M. Vargas, W.G. Chapman, Journal of Natural Gas Science and Engineering, 45 (2017) 738-746.
[37] J.B.G. Daldrup, C. Held, F. Ruether, G. Schembecker, G. Sadowski, Ind. Eng. Chem. Res., 49 (2010) 1395-1401.
[38] N.I. Diamantonis, I.G. Economou, Energy Fuels, 25 (2011) 3334-3343.
[39] F. Tumakaka, G. Sadowski, Fluid Phase Equilib., 217 (2004) 233-239.
[40] J.M. Prausnitz, R.N. Lichtentaler, E.G. de Azevedo, Molecular Thermodynamics of Fluid-Phase Equilibria, 3rd Edition, Prentice Hall, Upper saddle river, New Jersey, 1998.
[41] NIST, NIST Chemistry WebBook, NIST Standard Reference Database Number 69, National Institute of Standards and Technology, Gaithersburg, MD, 2019.
[42] M. Haruki, K. Kishimoto, F. Kobayashi, S.-i. Kihara, S. Takishima, J. Chem. Eng. Jpn., 42 (2009) 309-318.
[43] R. Paus, Y. Ji, L. Vahle, G. Sadowski, Mol. Pharmaceutics, 12 (2015) 2823-2833.
[44] A.C. Galvao, P.F. Arce, W.S. Robazza, T.D. Machado, C.A.L. Franca, Ind. Eng. Chem. Res., 59 (2020) 1319-1326.
[45] E.J. Roggeman, A.M. Scurto, J.F. Brennecke, Ind. Eng. Chem. Res., 40 (2001) 980-989.
[46] S. Poston, A. Reisman, J. Electron. Mater., 18 (1989) 79-84.
[47] M. daSilva, M.J.S. Monte, J. Huinink, J. Chem. Thermodyn., 28 (1996) 413-419.
[48] Y. Zhang, S. Wei, H.-H. Wang, J.-Q. Liu, W. Wang, J. Chem. Eng. Data, 62 (2017) 1292-1301.

[49] J. Gross, J. Vrabec, AlChE J., 52 (2006) 1194-1204.
[50] J. Gross, AlChE J., 51 (2005) 2556-2568.